Structure and Stability of a DNA Triple Helix in Solution: NMR Studies on $d(T)_6 \cdot d(A)_6 \cdot d(T)_6$ and Its Complex with a Minor Groove Binding Drug

Kimiko Umemoto,† Mukti H. Sarma, Goutam Gupta, Jia Luo, and Ramaswamy H. Sarma*

Contribution from the Institute of Biomolecular Stereodynamics, Department of Chemistry, State University of New York, Albany, New York 12222. *Received November 10, 1989*

Abstract: The possibility of both Watson-Crick and Hoogsteen A·T pairs can result in a triple helical structure for $d(T)_6 \cdot d(A)_6 \cdot d(T)_6$ in solution. In the triple helix the Watson-Crick paired T strand can run antiparallel, while the Hoogsteen paired T strand can run parallel to the A strand. On the basis of 1D/2D NMR studies, we have characterized the structural properties of the triple helix in terms of (a) nature of H-bonding, (b) chain conformations and relative chain orientations, (c) location of triplets T·A·T with respect to the helix axis, and (d) effects of NaCl and $MgCl_2$. In addition, we experimentally demonstrate that a minor groove specific drug Dst2 (a distamycin analogue) can bind to the triple helix. We show that the nature of thermal transition is altered by Dst2 binding; i.e., the host triple helix shows triple → coil (monophasic) transition in the absence of Dst2, while in its presence the helix shows a triplex → duplex → coil (biphasic) transition.

Over 30 years ago, in 1957, Felsenfeld et al.[1] reported a triple helical structure for poly[r(U)]·poly[r(A)]·poly[r(U)] based upon fiber diffraction analysis. This marked an important discovery in the field of DNA structure because this was the first suggestion that both Watson-Crick and Hoogsteen A·U pairs can be present in the same nucleic acid structure. Since then, for more than 15 years, a great deal of physicochemical study has been done to examine the spectroscopic and thermodynamic properties of synthetic triple helical polymers of nucleic acids.[2-4] However, during this time, very little work was done to study the intimate structural details of triple helical structures in DNA or to examine any biological relevance that these structural motifs might have. In 1974, the story of the triple helix was briefly revived. On the basis of fiber diffraction data for poly[d(T)]·poly[d(A)]·poly[d(T)], Arnott et al.[5] proposed a triple helical model; as in the case of its RNA counterpart (due to Felsenfeld et al.[1]), the third chain in the DNA triple helix runs parallel to the Watson-Crick A·T duplex and is stabilized by Hoogsteen A·T pairs. Arnott et al.[5] postulated that transient triple helix formation may be a possible mechanism by which the poly[d(A)] sequence is transcribed without breaking the template DNA duplex. Even after Arnott et al.[5] proposed the triple helix of DNA in 1974, understanding of this structure was no better than it was in 1957. This was due to the fact that both the 1957 and 1974 models of the triple helix were derived from poorly resolved fiber diffraction data. Models derived from fiber diffraction data provide no direct experimental proof for the presence of Hoogsteen A·T pairs in the same manner that single cocrystal structures[6,7] of A and T(U) do. It became obvious in the late 1970s that polymers are not the system of choice and that the fiber diffraction method is not the preferred technique to determine the fine structural details of a triple helix or for that matter any DNA/RNA system. The need for DNA/RNA oligomers of defined length and sequence and for an experimental tool that allows an easy probe into the structure and interactions of each constituent nucleotide in the oligomer became apparent. In the 1980s, with the emergence of automated DNA oligomer synthesizers and with the advent of 2D NMR spectroscopy, one is presented with the scope of an in-depth study of a triple helix. Hence, it is not surprising that recently there has been a reemergence of interest in the triple helix; i.e., attempts are being made to probe the intimate structural details and biological functions.

Moser and Dervan[8] were the first to rejuvenate interest in the field of DNA triple helixes. They showed that the triple helix could be used for sequence-specific recognition of DNA (a novel function that is 10^6 more specific than restriction enzymes). In this paper (1) the *orientation* of the Hoogsteen strand in the triple helix was documented for the first time and (2) the effect of *length, single-base mismatch, pH, role of organic cosolvent, added cations, oligonucleotide concentrations* and, importantly, *specificity* (ratio of sites bound) was first described. Lyamichev et al.[9] also demonstrated that triple helix formation facilitates the release of superhelical stress in the circular DNA. Recently, Rajagopal and Feigon[10] conducted solution NMR studies on $d(C^+T)_4 \cdot d(GA)_4 \cdot d(CT)_4$ at acidic pH and showed for the first time the presence of a triple helix and Hoogsten G·C$^+$ and A·T pairs. In our laboratory, as a part in our long-term interest in structure-function correlation of DNA oligomers of biological relevance, we focused our attention on the structure and dynamics of triple helices with A·T pairs. During the Sixth Conversation in Biomolecular Stereodynamics, June 1989, we reported[11] the stereochemical details of a triple helix with Watson-Crick and Hoogsteen A·T pairs, based upon 2D NMR studies on $d(T)_6 \cdot d(T)_6$ at neutral pH. At the same conference, in an independent effort, Pilch et al.[12] reported a triple helical structure for $d(T)_{10} \cdot d(A)_{10} \cdot d(T)_{10}$. In the present study, we not only demonstrate the presence of a triple helical structure for Na^+ and Mg^{2+} salts of $d(T)_6 \cdot d(A)_6 \cdot d(T)_6$ at neutral pH but also determine the conformations of the three strands. In addition, we compare the structural stability of the triple helix in the presence and absence of a minor groove binding drug.

* To whom correspondence should be addressed.
† Permanent address: Department of Chemistry, International Christian University, Mitaka, Tokyo 181, Japan.

(1) Felsenfeld, G.; Davies, D. R.; Rich, A. *J. Am. Chem. Soc.* **1955**, *79*, 2023.
(2) Brahms, J. *J. Mol. Biol.* **1965**, *11*, 785-801.
(3) Bloomfield, V. A.; Crothers, D. M.; Tinoco, I., Jr. *Physical Chemistry of Nucleic Acids*; Harper & Row: New York, 1974; pp 303-304.
(4) Morgan, A. R.; Wells, R. D. *J. Mol. Biol.* **1968**, *37*, 63-80.
(5) Arnott, S. A.; Selsing, E. *J. Mol. Biol.* **1974**, *88*, 509.
(6) Hoogsteen, K. *Acta Crystallogr.* **1963**, *16*, 907-916.
(7) Sobell, H. M. In *The Purines: Theory and Experiment*; Bergmann, E. D., Pullman, B., Eds.; The Israel Academy of Sciences and Humanities: Jerusalem, 1972; Vol. 4, pp 124-146.
(8) Moser, H. E.; Dervan, P. B. *Science* **1987**, *238*, 645.
(9) Lyamichev, V. I.; Mirkin, S. M.; Frank-Kamenetskii, M. D.; Cantor, C. R. *Nucleic Acids Res.* **1988**, *16*, 2165.
(10) Rajagopal, P.; Feigon, J. *Nature* **1989**, *339*, 637-640.
(11) Sarma, M. H.; Umemoto, K.; Gupta, G.; Sarma, R. H. *Book of Abstracts*, Sixth Conversation in Biomolecular Stereodynamics; Sarma, R. H., Ed.; Institute of Biomolecular Stereodynamics, SUNY at Albany, 1989; last page of the communication at the conversation site.
(12) Pilch, D. S.; Banville, D. L.; Shafer, R. H. *Book of Abstracts*, Sixth Conversation in Biomolecular Stereodynamics; Sarma, R. H., Ed.; Institute of Biomolecular Stereodynamics, SUNY at Albany, 1989; p 251.

0002-7863/90/1512-4539$02.50/0

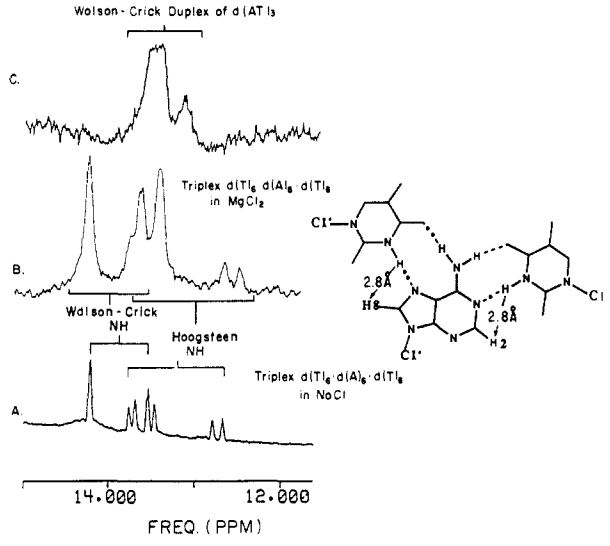

Figure 1. Imino proton NMR spectra of A·T containing oligomers in H_2O. (A) $d(T)_6 \cdot d(A)_6 \cdot d(T)_6$ in 100 mM NaCl at 3 °C; 0.5 mM in triple helix. (B) Imino region of the spectrum observed in H_2O for $d(T)_6 \cdot d(A)_6 \cdot d(T)_6$ at 1 °C in the presence of 20 mM $MgCl_2$. (C) $d(AT)_3$ at 1 °C; 0.5 mM in duplex. Note that the imino proton spectrum of $d(T)_6 \cdot d(A)_6 \cdot d(T)_6$ is quite different from that of $d(AT)_3$, which is considered to form a typical Watson–Crick A·T paired duplex. The temperature dependence of the spectrum of $d(AT)_3$ indicated that the peak centered at 13.5 ppm contains internal imino proton signals, while that at 13.2 ppm belongs to terminal protons. The peaks are shifted upfield compared to those of the Watson–Crick imino protons of $d(T)_6 \cdot d(A)_6 \cdot d(T)_6$ due to the difference in the stacking patterns in $d(AT)_3$ and $d(T)_6 \cdot d(A)_6 \cdot d(T)_6$. The imino protons are assigned on the basis of the NOE results and by comparison with the imino spectrum of $d(AT)_3$.

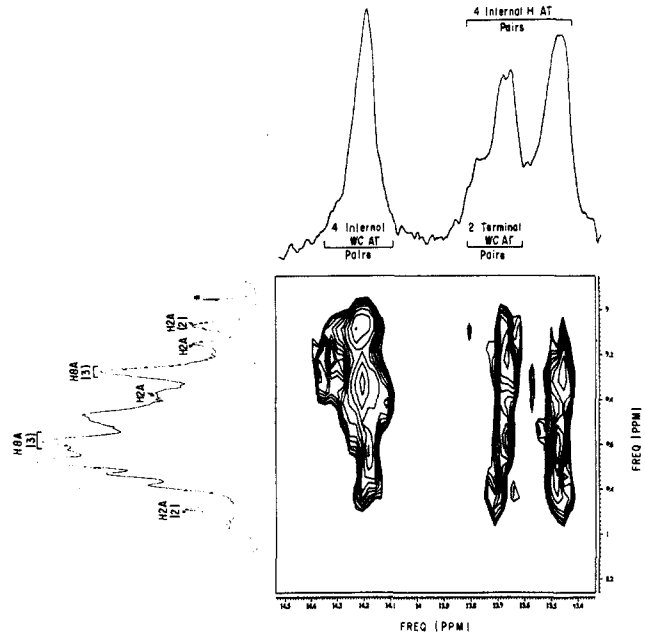

Figure 2. NOESY (τ_m = 200 ms) cross section of the Mg^{2+} (20 mM) salt of the triplex $d(T)_6 \cdot d(A)_6 \cdot d(T)_6$ in H_2O at 1 °C. Cross peaks between the imino protons (14.5–13.3 ppm) and the base protons (8.0–6.8 ppm) are shown. H2 of A, determined as the site of NOE from the imino protons of Watson–Crick A·T pairs, and H8 of A, determined as the site of NOE from the Hoogsteen A·T pairs, are shown. The imino region (12.8–12.6 ppm) corresponding to the terminal Hoogsteen A·T pairs is excluded from the cross section; one of these protons shows a weak cross peak with NH_2 of A. The 2048 × 512 data were collected in the phase-sensitive mode; NS = 96, RD = 1.5 s. In the 1D NOE experiment (τ_m = 500 ms), irradiation in the imino proton signals at 12.79 and 12.65 ppm from the terminal Hoogsteen A·T pairs shows H8 at 7.25 ppm as the only prominent site of NOE. Thus, H8 signals from the two terminal Hoogsteen A·T pairs are also located at 7.25 ppm (data not shown). The spike marked with an asterisk is a machine artifact.

Material and Methods

DNA Synthesis and Purification. The hexamers $d(A)_6$ and $d(T)_6$ were synthesized on a DNA synthesizer (Applied Biosystems Model 380A) following the method of Matteuci et al.[13] The product was purified on a 1.1 cm × 50 cm column of Q-Sepharose (Pharmacia) with a linear gradient of NaCl in 10 mM NaOH, 0–0.5 M NaCl for $d(A)_6$ and 0.5–1.2 M NaCl for $d(T)_6$. The distamycin analogue Dst2 was a generous gift from Drs. Z. Zhuze, A. Zaedatelev, and G. Gursky of the Institute of Molecular Biology, Academy of Sciences, USSR.

NMR Samples. For both H_2O and D_2O samples, the DNA concentration was 0.5 mM in $d(T)_6 \cdot d(A)_6 \cdot d(T)_6$ or in $d(AT)_3$. The solutions were prepared in 20 mM sodium phosphate buffer (pH 7.0) with 1 mM EDTA; two different salts were used, i.e., 100 mM NaCl and 10–20 mM $MgCl_2$. In the drug titration experiment, the distamycin analogue (Dst2; see inset of Figure 6) was added to an H_2O solution of $d(T)_6 \cdot d(A)_6 \cdot d(T)_6$ in increments of 0.25 molar equiv of the triplex.

NMR Spectroscopy. Proton NMR spectra were recorded at 500 MHz. Chemical shift values are given in ppm with respect to TSP as an internal standard. One-dimensional spectra in H_2O were taken at 1–20 °C, with a time-shared long pulse sequence. One-dimensional NOE spectra in H_2O were obtained for the presaturation time τ_m of 10–2000 ms with a relaxation delay (RD) of 2 or 1 s. NOESY spectra (τ_m = 100 and 250 ms) and MINSY spectra (τ_m = 250 ms) in D_2O were collected at 3 °C with the pulse sequence $[RD\text{–}90°\text{–}t_1\text{–}90°\text{–}\tau_m\text{–}90°\text{–}Acq]_{NS}$. The HDO signal was presaturated in the NOESY and MINSY experiments. The phase-sensitive NOESY spectra of $d(T)_6 \cdot d(A)_6 \cdot d(T)_6$ in H_2O (10 mM $MgCl_2$) were recorded on a GN500 machine with the pulse sequence of Skelnar et al.;[14] data size = 512 × 2048, NS = 96, RD = 1.5 s, and τ_m = 200 ms. Further suppression of H_2O was achieved by using spline base-line flattening of FIDs based upon the methods of Bielecki and Levitt[15] and Marion et al.[16]

Three-Dimensional Structure Generation Using Full-Matrix NOESY Simulation. The principle of full-matrix NOESY simulation developed by Keeper and James[17] is an elegant theoretical method to estimate NOEs for a proton pair in a given structure. In this method, the calculated NOEs contain contributions from both primary and higher order NOEs. Hence, it is not necessary to compute interproton distance from the observed data by assuming the presence of primary NOE alone because experimentally, even at the lowest τ_m, some small but finite contributions from higher order NOEs cannot be eliminated. Broido et al.[18] used this method for the first time to compute NOESY intensities for various cross peaks of a DNA oligomer in a given conformation. Previously,[19] we extended this method to select one of many stereochemically allowed duplex models; the selection of the model was judged by the best agreement between calculated and observed NOESY intensities. The agreement index of a structure is given by the R-factor = $1/N\sum(a^o_{ij} - a^c_{ij})/a^o_{ij}$, where a^o_{ij} and a^c_{ij} are the observed and calculated NOESY intensities for proton pairs (i,j) and N is the total number of (i,j) pairs considered. NOESY-constrained model building was done in the following manner. The NOESY and MINSY data suggested that T nucleotides on both strands in the triplex adopted a C3′-endo,anti conformation. Although there was no direct evidence from the MINSY data, the NOESY data were consistent with the C3′-endo,anti conformation of the A residues in the triplex. This meant that the range of values for δ should be within 70–100° and the range of values for χ should be within 190–230°. Stereochemical analysis of various B- and A-DNA crystals shows that the range of values for β is 150–210°, for γ the range is 40–70°, and for ϵ it is 170–220°. A linked-atom least-squares method[20] was used to generate the triplex with 10 T·A·T triplets per turn of the helix and an axial separation of 3 Å; the base-pairing scheme is as shown in Figure 1. The torsion angles α, β, γ, δ, ϵ, ζ, χ are treated as elastic variables with appropriate weights to stay within the observed range. Low weights are assigned to α and ζ so as to mimic an almost free rotation around the P–O bonds. The base parameters, i.e.,

(13) Matteuci, M. D.; Caruthers, M. H. *J. Am. Chem. Soc.* **1981**, *103*, 3185–3191.
(14) Skelnar, V.; Brooks, B. R.; Bax, A. *FEBS Lett.* **1987**, *216*, 249–252.
(15) Bielecki, A.; Levitt, M. H. *J. Magn. Reson.* **1989**, *82*, 562–567.
(16) Marion, D.; Ikura, M.; Bax, A. *J. Magn. Reson.* **1989**, *84*, 425–430.
(17) Keeper, J. W.; James, T. L. *J. Magn. Reson.* **1984**, *57*, 404–429.
(18) Broido, M. S.; James, T. L.; Jon, G.; Keeper, J. W. *Eur. J. Biochem.* **1985**, *150*, 117–128.
(19) Gupta, G.; Sarma, M. H.; Sarma, R. H. *Biochemistry* **1988**, *27*, 7909–7919.
(20) Arnott, S. A.; Dover, S. D.; Wonacott, A. J. *Acta Crystallogr.* **1969**, *B25*, 2192–2205.

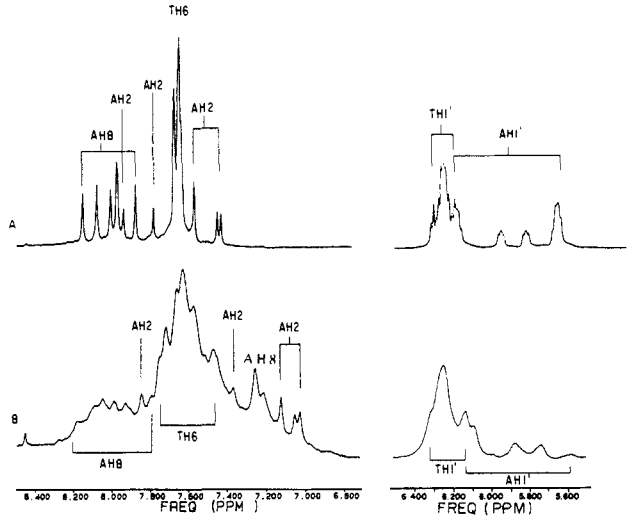

Figure 3. 1D NMR spectra observed in D_2O for base and H1′ protons of $d(T)_6$·$d(A)_6$·$d(T)_6$ in 100 mM NaCl at (A) 25 °C and (B) 3 °C. At 25 °C, $d(A)_6$ and $d(T)_6$ are single stranded. By lowering the temperature, the signals, especially those of A H8, become quite broad and some of the A H2 signals are shifted upfield by 0.3–0.4 ppm.

Table I. Chemical Shift Values of Various Proton Types[a]

	adenine	thymine
H8/H6	8.2–7.8	7.7–7.5
H2[b]/CH_3	7.8–7.7, 7.4–7.0	1.8–1.5
H1′	6.1–5.7	6.3–6.1
H2′, H2″	2.6–2.5, 2.9–2.5	2.4–2.3, 2.7–2.6
H3′	(hidden under HDO)	4.9

[a] Chemical shift values are given in ppm. [b] Comparison with the spectra of the Mg^{2+} salt suggests that one or two H8 signals may be located at 7.25 ppm.

base tilt, propeller twist, and base displacement, are also treated as variables.[21] This resulted in a series of stereochemically allowed triplex models with values of δ and χ in the desired range as expected from the NOESY and MINSY data. Full-matrix NOESY simulations were performed for the triplex models, taking into account all nonexchangeable base and sugar protons. The model that gave the lowest *R*-factor[19] was chosen as the most probable structure of the triplex. We have earlier shown[19] that full-matrix NOESY simulation can produce a reliable quantitative structure provided several well-resolved pairwise NOESY cross peaks can be experimentally obtained at all mixing times. In the case of the triplex, we are at a serious disadvantage because of the limiting number of experimentally observed pairwise NOESY cross peaks due to extensive overlap of the protons. Therefore, the triplex model proposed in this paper is not a rigorously quantitative structure.

For a discussion of the limitations of quantitative analysis of overlapping NOESY cross peaks and line-shape simulations, see refs 27 and 28.

Results and Discussion

Observation of Imino Signals from Watson–Crick and Hoogsteen A·T Pairs. A possible scheme of hydrogen bonding in a T·A·T triplet is shown in Figure 1 (inset); in this arrangement Watson–Crick paired A and T strands run antiparallel to each other while Hoogsteen paired A and T strands run parallel. The presence of Watson–Crick and Hoogsten A·T pairs can be detected by monitoring the imino signals in T (Redfield et al.[22] 1981; Geerdes et al.,[23] 1977). Figure 1A shows the 1D NMR spectrum of $d(T)_6$·$d(A)_6$·$d(T)_6$ in H_2O at 3 °C in the presence of 100 mM NaCl (pH 7.0). Note that, in addition to the imino protons of

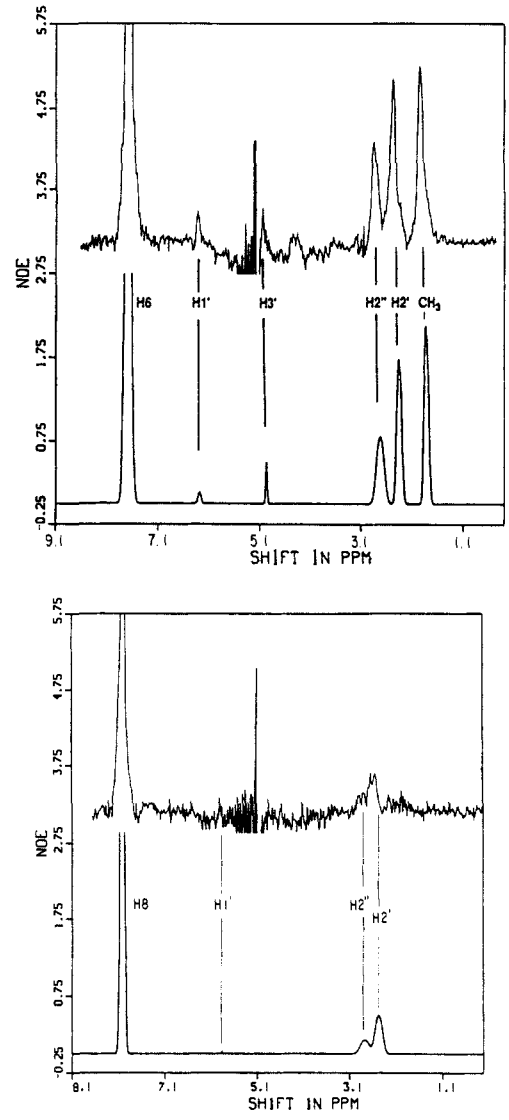

Figure 4. Representative (top) observed and (bottom) calculated (by simulation) NOESY slices for $d(T)_6$·$d(A)_6$·$d(T)_6$ through (A) T H6 and (B) A H8 at τ_m = 100 ms. Note that, from T H6, distinct NOE peaks are observed at H1′, H3′, H2″, H2′, and CH_3 protons, whereas from A H8, NOE peaks are hardly observable except for a broad H2″/H2′ peak.

Watson–Crick A·T pairs (expected within the 14.3–13.6 ppm range), a set of signals appear at 0.2–1.7 ppm higher field than the Watson–Crick signals. For $d(AT)_3$, capable of forming only a Watson–Crick A·T paired duplex, imino proton signals are located within 13.6–13.2 ppm (see Figure 1C); the imino signals from the internal A·T pairs are centered at 13.6 ppm, while those from the terminal ones are centered at 13.2 ppm. Thus, additional signals within 14.0–12.5 ppm in Figure 1A must originate from the Hoogsteen A·T pairs in the triple helix of $d(T)_6$·$d(A)_6$·$d(T)_6$, and the signal at 14.21 ppm should originate from the internal Watson–Crick A·T pairs. Figure 1B shows the imino signals of the triplex at 1 °C in the presence of 10 mM $MgCl_2$. Note that a triplex is also formed in the presence of $MgCl_2$ as evidenced by the presence of signals other than those of the Watson–Crick imino protons. Also note that Mg^{2+} causes a small change in the chemical shift values and in the shape of the imino signals as compared with the spectrum (Figure 1A) of the triplex in NaCl. In the presence of NaCl, seven well-resolved imino signals appear at 14.21, 13.76, 13.69, 13.52, 13.44, 12.79, and 12.65 ppm. In the presence of $MgCl_2$, the signals at 14.21, 12.79, and 12.65 ppm remain the same while the remaining four signals reshuffle or merge to appear at 13.76, 13.67, and 13.46 ppm. Note that the relative heights of the terminal Hoogsteen signals within 12.8–12.6 ppm in Figure 1, panels A and B, are different. This is due to the fact that these two spectra were recorded with two different

(21) For definition of torsion angles and base parameters refer to: Saenger, W. *Principles of Nucleic Acid Structures*; Springer-Verlag: New York, 1984.

(22) Redfield, A. G.; Roy, S.; Sanchez, V.; Tropp, J.; Figueroa, N. In *Proceedings of the Second SUNYA Conversation in the Discipline of Biomolecular Stereodynamics*; Sarma, R. H., Ed.; Adenine Press: Guilderland, NY, 1981; Vol. 1, pp 195–208.

(23) Geerdes, H. A. M.; Hilbers, C. W. *Nucleic Acids Res.* **1977**, *4*, 207–221.

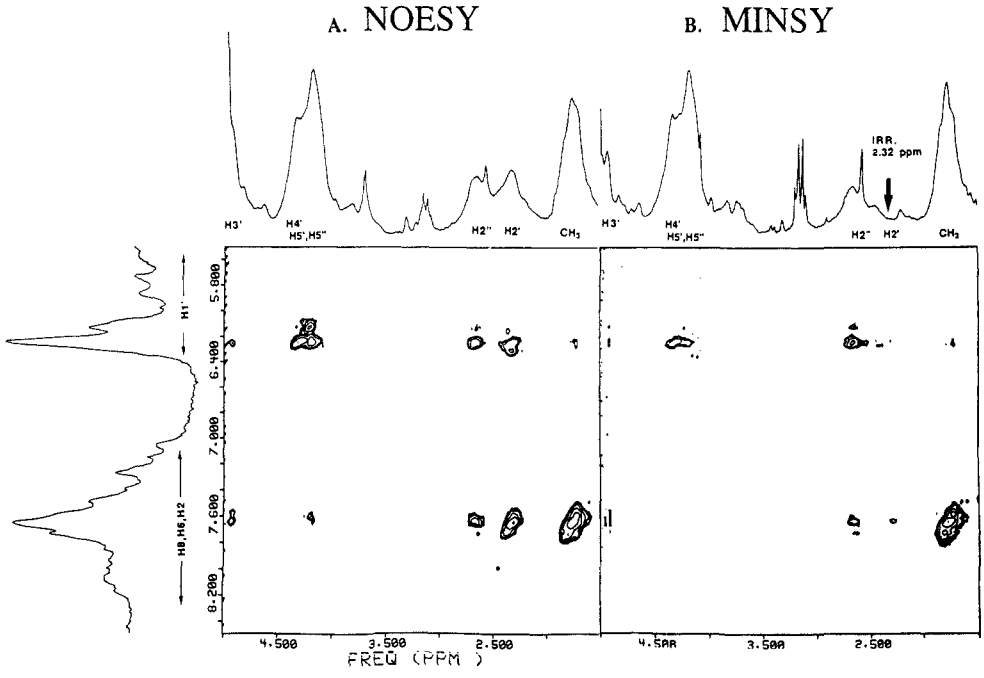

Figure 5. (A) NOESY and (B) MINSY cross sections involving base/H1′ protons and sugar protons (H2′, H2″, H3′, H4′, H5′, H5″, and CH_3) observed for $d(T)_6$·$d(A)_6$·$d(T)_6$ in 100 mM NaCl at 3 °C. For MINSY, the decoupler was placed at 2.32 ppm irradiating most of the H2′ signals of T. Note that the cross peak for T H6 (7.64 ppm)–T H3′ (4.92 ppm) is clearly observed in NOESY as well as in MINSY cross sections, indicating that they are primary NOEs. Also note that most of the cross peaks from A H8 and A H1′ are not observable mainly because of the broadness of these peaks. The presence of a moderately strong A H8–A H2′ NOE, however, rules out any possibility of a syn conformation for adenines in the A strand.

pulse sequences, i.e., a time-shared long pulse sequence for the spectrum in Figure 1A and the pulse sequence of Skelnar et al.[14] for the spectrum in Figure 1B.

A direct confirmation of the presence of Watson–Crick and Hoogsten A·T pairs is normally obtained by monitoring NOEs at H8 and H2 of A from the imino proton of T (Redfield et al.,[22] 1981). For a Watson–Crick A·T pair, a prominent NOE is expected at H2 of A from the imino proton of T, while for a Hoogsteen A·T pair, a NOE is expected at H8 of A (see inset of Figure 1). In order to demonstrate the presence of both Watson–Crick and Hoogsteen A·T pairs in the $d(T)_6$·$d(A)_6$·$d(T)_6$ triplex, we conducted NOESY (τ_m = 200 ms) and 1D NOE (τ_m = 500 ms) experiments in H_2O at 1 °C in the presence of 10 mM $MgCl_2$. Figure 2 shows the NOESY cross section involving the imino protons (14.5–13.4 ppm) and the base protons (8.5–6.8 ppm). From the imino protons of four internal A·T pairs, NOESY cross peaks are observed at 7.04 (two protons), 7.12 and 7.34 ppm; these signals are assigned to H2 of the four internal Watson–Crick A·T pairs in the triplex. The imino protons of the two terminal Watson–Crick A·T pairs overlap with the Hoogsteen A·T pairs in the region of 13.8–13.4 ppm; examination of the NOESY cross peaks from the signals within 13.8–13.4 ppm suggests that the H2 proton signals of the two terminal Watson–Crick A·T pairs are located at 7.85 ppm. The imino protons of the two terminal Hoogsteen A·T pairs, as concluded from the temperature profile (see later in the text, Figure 8A), are located at 12.79 and 12.65 ppm; weak NOESY (τ_m = 200 ms) cross peaks for these two signals appear within 7.47–7.42 ppm (data not shown); these cross peaks are assigned to the NH_2 of A because they disappear in the D_2O spectrum. The H8 resonance of the two terminal Hoogsteen A·T pairs is directly obtained from 1D NOE experiments. From 1D NOE (τ_m = 500 ms) experiments (data not shown), we are able to locate 7.25 ppm as the site of NOE from 12.79 and 12.65 ppm; therefore, we assign the 7.25 ppm signal to two H8 protons belonging to the two terminal Hoogsteen A·T pairs in the triplex. Cross peaks from the imino signals (13.8–13.4 ppm) of the four internal Hoogsteen A·T pairs are located within the broad region 7.65–7.59 ppm (three protons) and at 7.25 ppm. Thus, three H8 protons signals (of three internal Hoogsteen A·T pairs) are at 7.65 ppm, while three other H8 proton signals (of one internal and two terminal Hoogsteen A·T pairs) are at 7.25 ppm.

Results in Figure 2 clearly demonstrate the presence of both Watson–Crick and Hoogsteen A·T pairs in the triplex $d(T)_6$·$d(A)_6$·$d(T)_6$. We are also able to assign the chemical shift values for H8 and H2 of six A residues. Poor resolution of the signals does not permit us to make sequential assignment of H8 and H2 from these data. In addition to imino-H8/H6 cross peaks, we also observed imino-CH_3. Such cross peaks are also reported for $d(CGCGAATTCGCG)_2$ by Skelnar et al.[14]

Determination of Chain Conformations. Although the imino spectra in Figure 1A,B indicate the presence of both Watson–Crick and Hoogsteen A·T pairs vis-ā-vis a triple helical structure for $d(T)_6$·$d(A)_6$·$d(T)_6$, they do not provide any information regarding the conformations of A and T strands and their spatial relations in the triple helix. Conformations of the chains in terms of nucleotide geometry are obtained[19,24] by quantitative computer simulation of the NOE from base H8/H6 to sugar protons H1′, H2′, H2″, and H3′ as a function of mixing time τ_m. We carried out NOESY and MINSY experiments on the Na^+ and Mg^{2+} salts of the triplex.

Na^+ Salt of the Triplex. Figure 3 shows the base H8/H6/H2 and sugar H1′ region of $d(T)_6$·$d(A)_6$·$d(T)_6$ in the coil state at 25 °C (Figure 3A) and in the triple helical state at 3 °C (Figure 3B), both in the presence of 100 mM NaCl. Upon formation of a triple helix, two characteristic spectral features are observed: (1) All signals get broader, especially the H8's of A. (2) H2's of A are shifted by 0.3–0.4 ppm. The broadness of the signals in the present case did not permit sequencial assignment of the spin system routinely done from the NOESY data of DNA duplexes. However, we are able to isolate broad regions of the spectrum belonging to H8 of A, H6 of T, and corresponding sugar protons. NOESY data for $d(T)_6$·$d(A)_6$·$d(T)_6$ in D_2O at 3 °C for τ_m = 100 and 250 ms suggested the chemical shift (ppm) values of various proton types shown in Table I.

Several NOESY slices through broad regions of A H8 and T H6 are examined. Representative NOESY (τ_m = 100 ms) slices through A H8 and T H6 are shown in Figure 4. Note that, from T H6, distinct NOE sites are observed at H1′, H2′, H2″, H3′, and CH_3, while from A H8 a broad envelope appears, showing the NOE at the H2′, H2″ region. The nature of such a NOE

(24) Sarma, M. H.; Gupta, G.; Sarma, R. H. *Biochemistry* **1988**, *27*, 3423–3432.

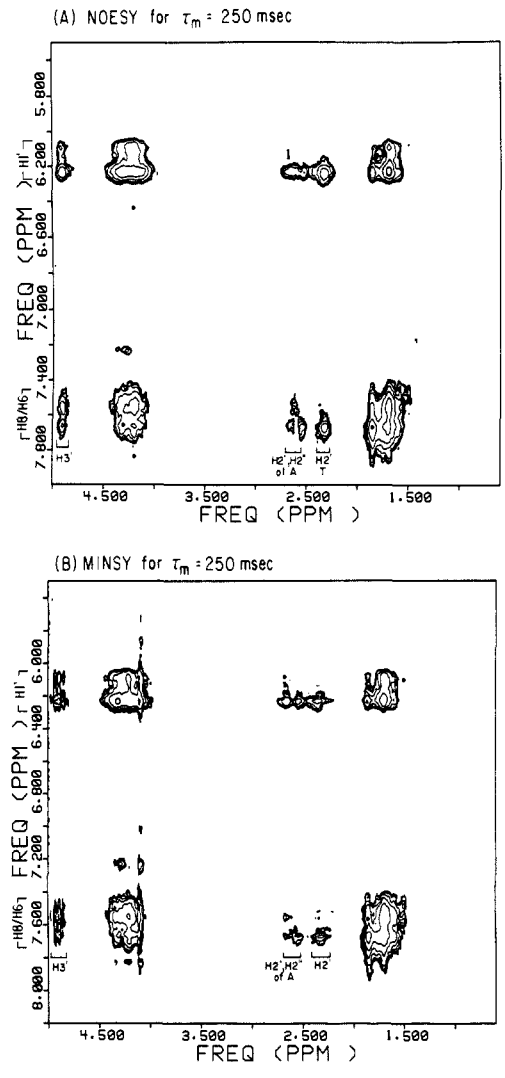

Figure 6. NOESY and MINSY spectra (τ_m = 250 ms) of the Mg^{2+} (20 mM) salt of the triplex $d(T)_6 \cdot d(A)_6 \cdot d(T)_6$ at 3 °C. In the MINSY experiment the signal at 2.3–2.2 ppm (H2′ of T) is irradiated to eliminate the H8/H6 → H2′ → H3′ diffusion pathway. Note the presence of H8/H6–H3′ cross peaks in the NOESY and MINSY spectra. In the MINSY experiment H2′ (T) signals within 2.3–2.2 ppm are not completely irradiated and hence they show a residual H6–H3′ cross peak, less intense than the corresponding peak in the NOESY spectrum. The relative intensities of H6–H3′ cross peaks in the NOESY and MINSY spectra are about the same; this suggests that the H6–H3′ NOE is a primary effect.

pattern from A H8 is due to the relative broadness of the corresponding signal. At τ_m = 100 ms, one essentially observes a primary NOE, and therefore, the presence of a T H6–T H3′ NOE indicates that T nucleotides may belong in the C3′-endo,anti domain, in which T H6–T H3′ distances are 2.7–3.3 Å. One alternative origin for the T H6–T H3′ NOE could be secondary effects, that is, T H6 → T H2′ → T H3′ as in the C2′-endo,anti nucleotide. In order to identify the true origin of the T H6–T H3′ NOE, we carried out a MINSY experiment on $d(T)_6 \cdot d(A)_6 \cdot d(T)_6$ in D_2O at 3 °C for τ_m = 250 ms following the procedure of Massefski and Redfield.[25] In the MINSY experiment, the decoupler is placed at 2.3 ppm to selectively irradiate T H2′ signals; as a result, the MINSY spectrum should show no T H6–T H3′ cross peak if the latter originated from secondary effects. But if the T H6–T H3′ NOE at τ_m = 100 ms is indeed a primary effect, MINSY data should show the T H6–T H3′ NOE. Figure 5B shows the MINSY cross section (τ_m = 250 ms) involving H8/H6/H2/H1′ versus H2′/H2″/H3′/H4′/H5′/H5″ protons. A NOESY cross section (τ_m = 100 ms) for the same region is shown for comparison in Figure 5A. Note the presence of a T H6–T H3′ cross peak in the MINSY cross section. Hence the data presented in Figure 5 and prove that T nucleotides in both the strands belong to the C3′-endo,anti domain. Signals for A H3′ being hidden under HDO prevented us from doing a similar examination of A H8 and A H3′ cross peaks.

Mg^{2+} Salt of the Triplex. NMR spectra of the triplex $d(T)_6 \cdot d(A)_6 \cdot d(T)_6$ in D_2O in the presence of 10–20 mM $MgCl_2$ show only a little change from the spectra in 100 mM NaCl. One notable change is the upfield shift of H8 from 8.2–7.9 ppm (in NaCl) to 7.7–7.5 ppm (in $MgCl_2$). We conducted NOESY experiments on the 20 mM Mg^{2+} salt of the triplex in D_2O at 3 °C for τ_m = 250 ms. The NOESY pattern bears a similarity with that of the Na^+ salt. We also performed MINSY experiments under the same conditions as for the NOESY experiment, with 2.2–2.3 ppm (the region belonging to H2′ of T) irradiated during mixing. Note that both NOESY and MINSY data (Figure 6) show cross peaks between H8/H6 and H3′. Thus, we conclude that in the presence of $MgCl_2$ both A and T residues adopt a C3′-endo,anti geometry. It may be pointed out that the signal at 7.25 ppm, where three H8's are located (two from terminal A's), shows a weak NOE with H2′; at the contour level of Figure 6 these cross peaks are not observed.

NMR data presented in Figures 1–6 suggest the following structural features of $d(T)_6 \cdot d(A)_6 \cdot d(T)_6$: (i) Watson–Crick and Hoogsteen A·T pairs are present in T·A·T triplets, as shown in the inset of Figure 1. (ii) T nucleotides in both strands have the C3′-endo,anti conformation, as deduced from the NOESY and MINSY data. Even though the nucleotide geometry of A nucleotides could not be inferred from A H8–A H3′ NOESY/MINSY cross peaks, the A H8–A H2′,H2″ NOE appears to be consistent with a C3′-endo,anti geometry of A. (iii) The C3′-endo,anti conformation of both T strands implies that the Hoogsteen paired T strand runs parallel to the A strands as shown in the inset of Figure 1; see refs 1 and 5 for explanations.

Molecular model building studies show that helix formation of T·A·T triplets displaces the bases away from the helix center; such a displacement is facilitated by the C3′-endo,anti conformation of A and T strands. Molecular modeling with the aid of full-matrix NOESY simulation resulted in a model of $d(T)_6 \cdot d(A)_6 \cdot d(T)_6$ that satisfies the structural criteria mentioned above. Figure 4 also shows theoretically constructed NOESY slices for A H8 and T H6 protons belonging to internal A and T residues in the structure. For the theoretical slices, NOESY intensities are obtained from the full-matrix simulation of the triple helical model and the theoretical NOESY absorption spectrum is generated by attributing appropriate line widths of various NOESY sites. Note the agreement between the observed and calculated spectra.

Figure 7A shows the stereopair of the triple helix of $d(T)_6 \cdot d(A)_6 \cdot d(T)_6$ viewed along the helix axis; the stacking arrangement of two successive T·A·T triplets is shown in Figure 7B. The NMR model in Figure 7 is only a qualitative model in which similar conformations are assumed for A and T residues. Poorly resolved NOESY/MINSY data (due to the very nature of the system) did not allow us to characterize the triple helix in terms of the conformation of each individual nucleotide.

NMR data on $d(T)_6 \cdot d(A)_6 \cdot d(T)_6$ are explained on the basis of a single major molecular species shown in the inset of Figure 1. However, for a small DNA oligomer (hexamer or octamer), the presence of minor molecular species cannot be ruled out[9] and they can cause complexity (line broadening of the signals, etc.) in the spectrum. The presence of minor molecular species in our system (not characterized even though not overlooked) does not alter our conclusions regarding the structure of the triple helix.

Effect of a Minor Groove Binding Drug, Dst2, on the Stability of the Triple Helix $d(T)_6 \cdot d(A)_6 \cdot d(T)_6$. In principle, the $d(T)_6 \cdot d(A)_6 \cdot d(T)_6$ triple helix can show either of the two temperature-induced structural transitions, i.e., a biphasic transition involving triple helix → double helix → coil or a monophasic one involving triple helix → coil. In the present system, it is possible to identify the mode of transition simply by monitoring the imino signals as

(25) Massefski, W., Jr.; Redfield, A. G. *J. Magn. Reson.* **1988**, *78*, 150–155.

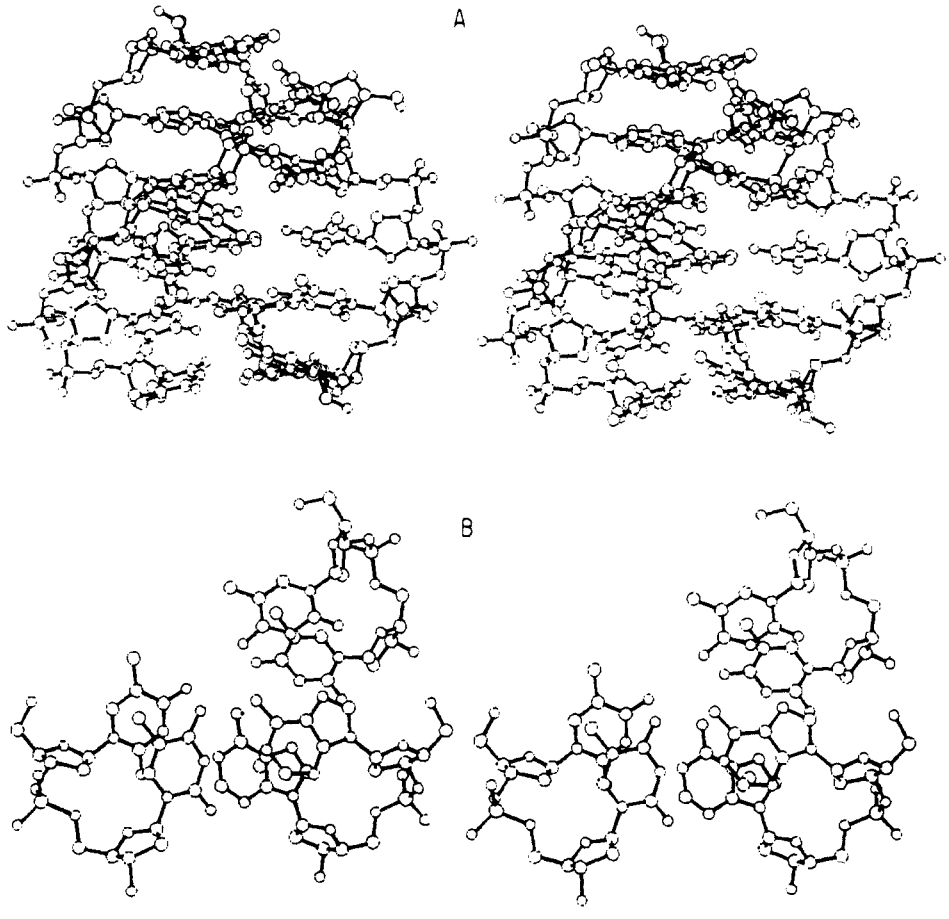

Figure 7. A stereoview of the $d(T)_6 \cdot d(A)_6 \cdot d(T)_6$ triple helix structure that is compatible with the NOESY pattern observed. (A) A view of the triple helix projected along the helix axis. (B) The stacking arrangement of two successive triplets, T·A·T. Note that the bases are moved away from the helix center. Such a displacement is a consequence of the simultaneous presence of Watson–Crick and Hoogsteen pairing and is facilitated by the C3′-endo,anti conformation of A and T residues.

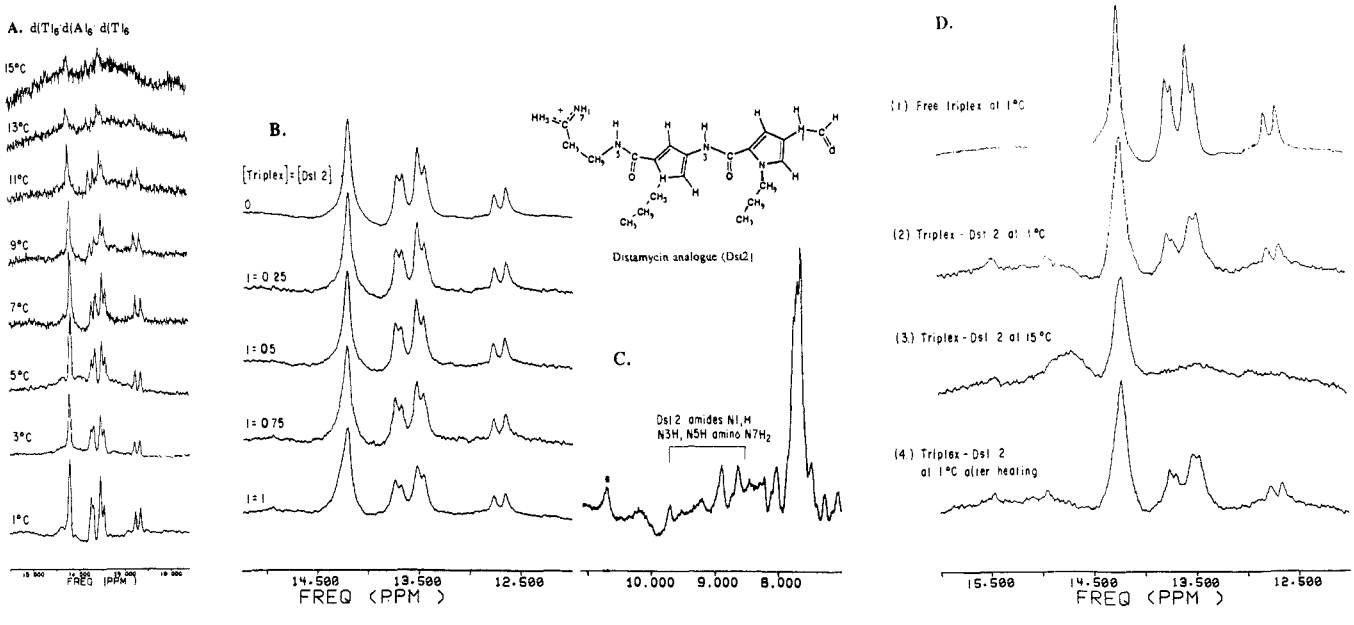

Figure 8. (A) Temperature dependence of imino proton signals of $d(T)_6 \cdot d(A)_6 \cdot d(T)_6$. Note that all the NH signals almost disappear at about 15 °C. (B) The NH signals observed during titration by a distamycin analogue (Dst2; see inset). Dst2 was added to the triplex $d(T)_6 \cdot d(A)_6 \cdot d(T)_6$ solution at 1 °C. Note that no marked effect is observed on the imino proton signals by the complex formation except for a slight broadening of the peaks. (C) In the region 8.5–9.8 ppm, however, signals from amino and amide protons of Dst2 H-bonded to the triplex started to appear as Dst2 was added, showing that the complex was formed. The peak marked with an asterisk most likely belongs to the other amino protons located on the convex surface of Dst2. (D) When the solution of triplex–Dst2 complex is heated to 15 °C, the T strand that formed Hoogsteen pairs in the complex apparently separates out, leaving a Watson–Crick duplex–Dst2 complex. (1) Free triplex at 1 °C. (2) Triplex–Dst2 complex at 1 °C. (3) Triplex–Dst2 complex at 15 °C. (4) Triplex–Dst2 complex, regenerated when the temperature is lowered to 1 °C after having been heated to 15 °C.

a function of increasing temperature. If the imino protons of the Hoogsteen A·T pair disappear at a temperature lower than those of the Watson–Crick A·T pairs, the transition is biphasic, and if the imino protons of both Hoogsteen and Watson–Crick A·T pairs disappear at the same temperature, the transition is monophasic. Figure 8A shows the temperature profile of the imino protons of Hoogsteen and Watson–Crick A·T pairs of $d(T)_6$·$d(A)_6$·$d(T)_6$ in H_2O. Note that all imino protons disappear at the same rate with temperature and, hence, the transition is truly monophasic.

In poly[d(T)]·poly[d(A)]·poly[d(T)], one observes a biphasic transition at a low $MgCl_2$ concentration and a monophasic transition at higher $MgCl_2$ concentrations.[26] It appears that, for polymers at low salt, the Hoogsteen pair of the triple helix is less stable than the Watson–Crick part, and thus there are two thermodynamically distinct domains in the triple helix showing a biphasic transition. This is due to the fact that, at low salt concentrations, two parallel chains in the Hoogsteen part show higher P–P electrostatic repulsion (closer proximity) than those in the Watson–Crick part of the triple helix. At higher salt concentrations, due to more effective screening of electrostatic P–P repulsion, both the Watson–Crick and Hoogsteen parts of poly[d(T)]·poly[d(A)]·poly[d(T)] become equally stable and hence the triple helix, being one thermodynamic entity, shows a monophasic transition. In the hexamer $d(T)_6$·$d(A)_6$·$d(T)_6$ system (at 100 mM NaCl), a monophasic transition indicates that the triple helix does not have two thermodynamically distinct entities in the Hoogsteen and Watson–Crick parts of the triple helix.

We have shown elsewhere[27] that a minor groove specific drug, Dst2 (a distamycin analogue shown in the inset of Figure 8B), specifically binds to Watson–Crick A·T pairs in the minor groove. It was of importance to examine if Dst2 can specifically bind to the Watson–Crick part of the triple helix. Figure 8B shows the Dst2 titration profile of $d(T)_6$·$d(A)_6$·$d(T)_6$ at 1 °C. The presence of amide/amino protons in the spectra (shown in Figure 8C for triple helix:drug 1:1 ratio) provides direct evidence of drug binding to the triple helix. Stereochemically, Dst2 has a distinct preference for binding (and stabilizing) Watson–Crick over Hoogsten A·T pairs, because for a Watson–Crick A·T pair N3 A and O2 T in the minor groove are participants in H-bonding with the drug amide protons (see Figure 8**B**), while for a Hoogsteen A·T pair only O2 T is available in the minor groove to form H-bonds with the drug amide protons. Consequently, Dst2 binding to the triple helix should create two thermodynamically distinct domains in the triple helix $d(T)_6$·$d(A)_6$·$d(T)_6$, and the temperature-induced transition of the complex should be biphasic. The temperature profile of the triple helix–Dst2 complex (Figure 8D) does indeed reveal a biphasic transition. At 15 °C, the imino protons of the Hoogsteen A·T pairs disappear, while the Watson–Crick A·T pairs disappear at 20 °C (data not shown). Note that, upon cooling from 15 to 1 °C, the Watson–Crick duplex–Dst2 complex gets reconverted to a triplex–Dst2 complex (Figure 8D). This is a clear demonstration that Dst2 can bind the preformed $d(T)_6$·$d(A)_6$·$d(T)_6$ triplex. The fact that the Hoogsteen imino protons of the free and drug-bound triplex disappear at the same temperature shows that the drug Dst2 does not destabilize the triplex.

(26) Riley, M.; Maling, B.; Chamberlin, M. J. *J. Mol. Biol.* **1966**, *20*, 359–389.
(27) Sarma, M. H.; Gupta, G.; Garcia, A. E.; Umemoto, K.; Sarma, R. H. *Biochemistry*, in press.
(28) Umemoto, K.; Sarma, M. H.; Gupta, G.; Sarma, R. H. *Biochemistry*, in press.

Summary

In this paper, we have provided NMR data to show that $d(T)_6$·$d(A)_6$·$d(T)_6$ in solution at 3 °C (for either the Na^+ or Mg^{2+} salt, pH 7) forms a triple helical structure. Both Watson–Crick and Hoogsteen A·T pairs are present in this structure. We have also determined the average conformations of nucleotides in the three chains and their relative orientations; i.e., nucleotides in the A and T strands belong to the C3′-endo,anti domain and the Watson–Crick T strand runs antiparallel while the Hoogsteen paired T strand runs parallel to the A strand. Our NMR model of the triple helix $d(T)_6$·$d(A)_6$·$d(T)_6$ is close to that proposed by Felsenfeld et al.[1] and Arnott and Selsing[5] for polymeric DNA and RNA. A novel observation is made regarding the structural stability of the triple helix $d(T)_6$·$d(A)_6$·$d(T)_6$ in the presence of a minor grove binding drug, Dst2. In the absence of Dst2, $d(T)_6$·$d(A)_6$·d(T)6 shows a temperature-induced triple helix → coil (monophasic) transition. In the presence of Dst2, preferential drug binding to the Watson–Crick part (and consequent stabilization) makes the transition biphasic, i.e., triple helix → duplex → coil.

Acknowledgments. This research is supported by grants from the National Institutes of Health (GM37812, GM29787) and by a contract from the National Foundation for Cancer Research. The high-field NMR experiments were performed at the NMR Facility for Biomolecular Research located at the F. Bitter National Magnet Laboratory, MIT. The NMR facility is supported by Grant RR00995 from the Division of Research Resources of the NIH and by the National Science Foundation under Contract C-670. This work is also supported by the U.S. Department of Energy. K.U. thanks the International Christian University, Tokyo, Japan, for granting a sabbatical leave. NOE experiments in H_2O and subsequent data processing were performed at the NIH Resources for Multinuclear NMR and Data Processing at Syracuse University. The resource is supported jointly by the Biomedical Research Technology Program of the Division of Research Resources of NIH (Grant RR1317) and by Syracuse University.

Registry No. A, 73-24-5; T, 65-71-4; $d(T)_6$·$d(A)_6$·$d(T)_6$, 126788-53-2; Na, 7440-23-5; Mg, 7439-95-4; distamycin analogue, 75656-22-3.